



FABRICATION AND CHARACTERIZATION OF POTENT BIOLARVICIDE SYNTHESIZED FROM METALLIC NANOPARTICLES USING LEAVES OF *TINOSPORA CORDIFOLIA*

¹ M. Malliga devi ² R.Rajeswari Anburaj*,

¹Axon drug private limited, Chembarapakkam, Chennai

²Assistant Professor, V.V.V College for Women, Department of Biotechnology,
Affiliated to Madurai Kamaraj University, Virudhunagar-626 001, TamilNadu, India

ABSTRACT

Green synthesis of AgNPs has been reported as safe, low cost and ecofriendly. This methodology uses extracts originating from different plants to reduce silver ions from AgNO₃ into nano-sized particles. Bioactive constituents present in plants were analysed by means of phytochemical analysis. Surface Plasmon peak at 430 nm confirms the presence of silver nanoparticles. The presence of the plant-origin capping agents surrounding AgNPs was proven by Fourier-transform infrared spectroscopy. Microbicidal potential of synthesized AgNPs using *T. cordifolia* suggest that 400µl, 300 µl was resistant against *B.subtilis*(22.5 mm), whereas least inhibition was found against *K. pneumoniae*(14.5 mm), *M. luteus*(13 mm). Therefore results suggest that *T. cordifolia* act as a potent larvicide and it is a suitable plant for the development of novel natural insecticides.

Keywords: Green reactants, capping agents, phytofabricated, microbicidal assessment, biolarvicide

I. Introduction

Nanoparticles have recently gained considerable attention in many fields such as medicine, electronics, food, agriculture, and energy [1]. Silver nanoparticles (AgNPs) can be produced either chemically or biologically [2]. Generally, conventional physical and chemical methods seem to be very expensive and hazardous. Interestingly, biologically-prepared AgNPs show high yield, solubility, and high stability [3]. One of the green nano-factories for synthesis and production of metal nanoparticles are microbes [4]. Recently, many strains of bacteria, such as *Bacillus sp.* and *Pseudomonas sp.*, and actinomycete have been used to convert silver ions to silver nanoparticles through the reduction process [5,6]. AgNPs have been proven as efficient metallic nanoparticles due to their promising bioactivities that can include antioxidant,[7] antifungal,[8] antibacterial [9] and anticancer properties [10]. The lethal activity of nanoparticles against broad spectrum of Gram-positive bacteria, Gram-negative bacteria and fungi has been approved [11]. The ion Ag that interacts with the cell prevents protein synthesis, further decreases the membrane permeability, and eventually leads to cell death [12].

Actinomycetes are considered a important resource for new products of medical and industrial interest such as antimicrobial agents [13,14]. They are being used as ecofriendly Nanofactories [15]. Actinomycetes are efficient candidates for metal nanoparticles production extracellularly and intracellularly. The synthesis of biofabricated nanoparticles by actinomycetes signify good stability and polydispersity. Actinomycetes acquire significant biocidal action against different pathogens.

Mosquitoes have always been a human health threat, major health problems caused by them are malaria, dengue fever, yellow fever, and Zika as well as several other vector-borne diseases [16]. According to data from the World Health Organization, the number of people affected with dengue in 2015 was 3.2 million, with 500,000 people hospitalized per year [17]. In the current situation, only physical and chemical methods are being used to control mosquito-borne diseases. Physical methods such as mosquito bed nets, mosquito window nets at homes, and electrical mosquito rackets are only temporary solutions.¹⁹ Vector control is done by means of chemicals diflubenzuron, and the control of adult mosquitoes with alpha-cypermethrin, deltamethrin, malathion, and others according to recommendations of the WHO Pesticide Evaluation Scheme,[18]. Unlike current synthetic or chemical insecticides, the advantages of plant-based insecticides are their compositions of natural blends of multiple chemical compounds that may act synergistically on both physiological and behavioral processes of mosquitoes [20-22]. Therefore, plant-based insecticides are a substitute and precise solution against dengue vectors of *Aedes aegypti*.

T. cordifolia (Willd.) is commonly known as Guduchi, Giloy or Heart-leaved Moonseed is a genetically different, large, transitory climber shrubs belong to menispermaceae family, [23,24]. Guduchi is widely used in Ayurvedic system of medicine “*Rasayanas*” to the immune system and body resistance against infections. In modern medicine it is used for general weakness [25]. The plant has several therapeutic properties such as jaundice, rheumatism, urinary disorder, skin diseases, diabetes, anemia, inflammation, allergic condition, anti-periodic properties etc [26]. This biological activities of the plant is due to its chemical constituents like diterpenoid glycosides, steroids, sesquiterpenoid, phenolics, essential oils and polysaccharides and is present in a diverse part of the plant body, including root, stem, and whole part [27]. The extract reversed the behavior of the target MPTP-intoxicated mice and it suggests that *T. cordifolia* protected dopaminergic neurons by suppressing neuro-inflammation in MPTP-induced Parkinsonian mouse model [28].

In the present study, green synthesis methods involve plants and microbes in synthesis of AgNPs. The biosynthesized nanoparticle can act as a potent larvicide showing inhibitory action against *Aedes aegypti* vectors.

II. EXPERIMENTAL SECTION

2.1 Chemicals and reagents used

Silver Nitrate (AgNO_3) and solvents like methanol and media such as nutrient agar were purchased from Sigma Aldrich, USA. All other reagents, chemicals and solutions used were of analytical grade.

2.2 Preparation of plant material

Tinospora cordifolia was collected from local surroundings of Madurai region. Fresh leaves were used for the extraction of active components were shade dried at room temperature and powdered using electrical blender. These pulverized samples were collected in an air sealed container.

2.3 Qualitative phytochemical examination

The dried leaves of plant material were successively extracted with methanol and kept in shaker for 2 days. The solvent was evaporated using rotary evaporator under reduced pressure at 37 °C. The plant extract was subjected to phytochemical analysis by the method described by Harborne [29]. The extract was screened for the presence of bioactive compounds like alkaloid, flavonoid, glycosides, phenol, saponin, steroid, tannin and terpenoids.

2.4 Biosynthesis of silver nanoparticles

Aqueous solution (1 mM) of silver nitrate (AgNO_3) was prepared and used for the synthesis of AgNPs. 5 ml of *T. cordifolia* along with 95 ml of aqueous solution of 1 mM AgNO_3 was mixed for reduction into Ag^+ ions. In a 250 ml conical flask 1.5 ml of leaf extract was added to 30 ml of 10^{-3} M AgNO_3 aqueous solution, this solution was kept in a water bath at 75 °C for 60 min. Bioreduction of Ag ions was experimented by means of brownish colour and analysed using spectrophotometric determination. The product was redispersed in deionized water and the centrifugation was continued constantly for two to three times to remove the absorbed substances on the surface of nanoparticles [30].

2.5 Microorganisms

Bacteria such as *Escherichia coli*, *Bacillus subtilis*, *Klebsiella pneumonia*, *Pseudomonas aeruginosa*, *Staphylococcus aureus*, *Mycobacterium luteus* were obtained from GH hospital, Madurai. The bacterial cultures were preserved on nutrient agar slants at 4 °C. The bacterial cultures were inoculated into nutrient broth and incubated for 24 h at 37 °C. The growth was compared with 0.5 McFarland; the turbidity of the medium indicates the growth of organisms [31].

2.6 Antimicrobial assay of silver nanoparticles

The AgNPs synthesized from *Tinospora cordifolia* were tested for antimicrobial activity by well-diffusion method against pathogenic microbes. According to Cheesbrough standard agar well diffusion method was engaged to identify the potential of AgNPs against the microbial isolate [32]. For microbicidal assay of the compounds, wells were made in plates containing nutrient agar medium seeded with 100 µl of 24 h of each microbial isolate. The wells were loaded with *T. cordifolia*, AgNO₃ and plant based synthesized silver nanoparticle was loaded using a micropipette. From each solution, that contains both Ag and *T. cordifolia* extracts, as well as the control, synthesized silver nitrate was placed in separate wells. AgNO₃(200µl) solution was used as a standard to determine their inhibition potential. The plates were left in refrigerator for 2 h then incubated at 37 °C for 24 h. The diameter of inhibition zones was calculated and tabulated by comparing with standard.

2.7 Larvicidal bioassay:

The Larvicidal activity of green synthesised silver nanoparticle using *T. cordifolia* was assisted by the procedure of WHO as per the modification of Rahuman *et al.*, [33] The plant extract and the silver nanoparticle solution was prepared as mentioned in antibacterial assay. For this bioassay test, larvae were taken in 3 batches of 25 in 99 ml dechlorinated tap water. 1ml of *T. cordifolia* extract is added in different concentration (250 ppm, 500 ppm, 750 ppm, 950 ppm, 1200 ppm) to the water prior to introduction of larvae. For Larvicidal bioassay of silver nanoparticle, 5 different concentration (250 - 1200 ppm) of silver nanoparticle solution is added to each cups. Sonication is done for the silver nanoparticle solution to avoid settling of silver nanoparticle in higher concentration prior to introduction of larvae. Control was maintained with dechlorinated tap water. The numbers of dead larvae were counted after 24 hours and 48 hours of exposure. And the percentage of mortality was reported from the average of replicates. The mortality is calculated by **Abbot's formula**.

$$\text{Corrected mortality} = \frac{\text{Observed mortality in treatment} - \text{Observed mortality in control}}{100 - \text{control mortality}} \times 100$$

$$\text{Percentage mortality} = \frac{\text{Number of dead larvae}}{\text{Number of larvae introduced}} \times 100$$

2.8 Statistical analysis:

All the data were subjected to statistical analysis by Probit analysis by finney [34].

2.9 Actinomycetes

From collected sample, 5g of the soil were suspended in 50ml of Normal saline (NaCl 0.85g/L). The soil suspension were incubated in an orbital shaker incubator at 28°C with shaking at 200 rpm for 3 min. Actinomycetes were isolated by spread plate techniques following the serial dilution of soil. The following mediums were used for the isolation of Actinomycetes Starch casein agar medium, Water-yeast extract-agar (WYE), Actinomycetes Isolation Agar media. Isolated plates were incubated at 28°C for 7-15 days for fast growing Actinomycetes. Plates were checked for the growth of typical Actinomycetes colonies up to 7 days [35].

2.10 UV-Vis spectroscopy

The synthesized AgNP were observed visually for any colour change and one ml of reaction mixture were withdrawn consecutively at various time levels by diluting a small aliquot (100 µl) of the sample 10-fold in deionized water for analysis of surface plasmon resonance of silver nanoparticles. The reduction of pure Ag⁺ ions was monitored by measuring using a UV-Vis spectrophotometer (Shimadzu 1601 model, Japan) at the resolution of 1 nm in range of 200–800 nm.

2.11 FT-IR analysis

The functional groups of the nanoparticles were qualitatively confirmed by using FTIR spectroscopy, with spectra recorded by a Perkin-Elmer Spectrum 2000 FTIR spectrophotometer. Along with 300 mg of dried KBr, 3 mg of lyophilized sample, was mixed and compressed well in mortar and pestle to organize thin pellet for examination. Scans per sample were performed in range of 400–4000 cm⁻¹ [36].

2.12 Scanning electron microscopy (SEM)

The structure and composition of freeze-dried purified silver particles were analyzed by using a 10-kV ultra-high resolution scanning electron microscope. Purified silver nanomaterials after recurring centrifugation was sputter coated on carbon layered copper grids and the images of nanoparticles were studied using FEI QUANTA-200 SEM.

III. Results and Discussion

Table 1: Phytoconstituents in *T. cordifolia*

Phytoconstituents	Methanol
Alkaloid	+
Flavanoid	+
Saponin	-
Tannin	+
Phenol	+
Glycosides	+
Terpenoid	+
Steroid	+

The results of preliminary phytochemical evaluation of *T. cordifolia* were represented in Table: 1. Methanol extract remained positive towards alkaloid, flavanoid, tannin, phenol, terpenoid, whereas saponin was absent. Bioactivity of the plant is due to its chemical constituents present in different parts of the plant [37].

Table 2: Microbicidal efficacy of plant mediated AgNPs

Microorganism	<i>T.cordifolia</i> Zone of inhibition in mm				
	100µl	200 µl	300 µl	400 µl	Agno ₃ solution (200 µl)
<i>B. subtilis</i>	18±0.1	20.5±0.3	21.4±0.4	22.5±0	20±0
<i>E.coli</i>	16±0	17.3±0.4	18.4±0.2	20.1±0.1	18.6±0.2
<i>K. pneumoniae</i>	14.5±0.3	15.7±0.1	17±0	18.4±0.4	16±0
<i>M. luteus</i>	13±0	14.1±0.2	15.7±0.1	16.5±0	15.4±0.3
<i>P.aeruginosa</i>	14.6±0.1	16.5±0	18.4±0.2	19.4±0.3	17.5±0.3
<i>S. aureus</i>	17.5±0	19.3±0.3	20.5±0	21.3±0.2	19.5±0

3.1 Microbicidal potential of plant mediated AgNPs

Microbicidal assessment of plant assisted AgNPs were depicted in Table: 2. The antimicrobial potential of silver (Ag) and zinc oxide (ZnO) has been enhanced on a nanoscale, and they can be utilized to manage different human and animal pathogens with nanotechnology [38-44]. 400 µl of AgNP remained resistant towards *B. subtilis*(22.5 mm), followed by 300 µl of AgNP against *B. subtilis* (21.4 mm) and *S. aureus*(20.5 mm). Zhang et al. (2016) reported that the smaller size of AgNPs could cause more toxicity to the bacteria and show better bactericidal effect compared to the larger particles as they have larger surface area [45]. Moderate inhibitory effect was found to be observed in 200 µl against *E.coli*(17.3 mm), *P.aeruginosa*(16.5 mm). Microbicidal potential of AgNPs against multidrug resistant bacteria have been considered by many experimentation and it was proved that AgNPs are effective against multidrug resistant bacteria such as multidrug resistant *E. coli* [46] and methicillin resistant staphylococcus aureus [47] Minimum inhibition was found to be observed in *K.pneumoniae*(14.5 mm) and *M. luteus*(13 mm). The aqueous extract of *T. cordifolia* showed potent activity against *A. fumigates*, *Aspergillus flavus* and *Aspergillus niger* (fungus) in the study [48].

Table: 3 Larvicidal activity of aqueous & synthesized silver nanoparticles using *T. cordifolia* against fourth instar larvae of *Aedes species*

Extracts	Species	Concentration (mg/ppm)	Percentage mortality±SD	Lc ₅₀ (mg/ml) (LCL-UCL)	Lc ₉₀ (mg/ml) (LcCL-UCL)	slope	X ² (df-4)
Plant extract	<i>T.cordifolia</i>	500	95±0.930	10.799(2.732-12.614)	73.101(20.101-103.206)	0.93	0.971
		400	86±0.159				
		300	79±0.279				
		200	73±0.683				
		100	55±0.259				
Synthesized AgNPs		500	95±0.293	20.008(7.113-2.129)	10.287(4.507-13.812)	0.469	0.135
		400	93±0.239				
		300	87±0.119				
		200	79±0.687				
		100	63±0.704				

3.2 Mosquitocidal assay of *T.cordifolia*

Larvicidal activity of *Aedes* was evaluated against biosynthesized AgNP using *T.cordifolia* was represented in Table: 3. Plants have several bioactive compounds that are necessary for their survival against attacks by herbivorous pathogens and animals [49]. LC₅₀ of biofabricated AgNP using *T. cordifolia* was maximum(20.008), whereas the plant extract possess minimum(10.799)value. Similarly LCL value was found to be higher(7.113) in plant assisted AgNP, compared to plant(2.732), whereas the UCL value was found to be elevated in plant(12.614) extract, compared to synthesized AgNP(2.129). Slope acquired maximum level in biosynthesized AgNPs(0.469) compared to plant extract(0.93). X² values was found to be higher in plant (0.971), compared to synthesized AgNP (0.135).

Table: 3 Larvicidal activity of aqueous & synthesized silver nanoparticles using *actinomycetes* against fourth instar larvae of *Aedes species*

Extracts	Species	Concentration (mg/ml)	Percentage mortality±SD	Lc ₅₀ (mg/ml) (LCL-UCL)	Lc ₉₀ (mg/ml) (LcCL-UCL)	slope	X ² (df-4)
Culture extract	Actinomycetes	500 400 300 200 100	91±0.779 86±0.546 67±1.139 60±0.876 48±1.048	11.491(5.848-16.236)	115.746(38.738-153.44)	0.826	2.510
Synthesized AgNPs	Actinomycetes	500 400 300 200 100	96±0.394 92±0.761 80±0.640 72±1.168 60±1.208	2.089(10.396-12.587)	60.2333(25.626-19.379)	0.209	1.446

3.3 Mosquitocidal assay of *Actinomycetes*

Larvicidal activity of *Aedes* was evaluated against biosynthesized AgNP using actinomycetes was represented in Table: 4. The results of this study have shown that the phytochemical compounds extracted from *T. cordifolia* leaves may have innovative and integrated property of a bio insecticidal agent. LC₅₀ of actinomycete culture was maximum(11.491) compared to biofabricated AgNPs(2.089) using actinomycete, whereas LCL value of biofabricated AgNP was higher(10.396) compared to actinomycete culture(5.848). UCL value of actinomycete culture possess higher(16.236) value compared to synthesised AgNP(12.587) using actinomycete. Slope value was found to be elevated(0.826) in actinomycete culture, whereas

declined(0.209) in synthesised AgNP. X^2 value was found to be maximum(2.510) in actinomycete culture compared to synthesised AgNP(1.446). Thus, this study aims to emphasize the role of the extract as a substitute control measure against Aedes when compared to the synthetic insecticides.

Isolation of Actinomycetes



3.4 Appearance of Actinomycete

The actinomycete were isolated by means of serial dilution technique by spread plate method using Actinomycetes agar(Hi media) and the colonies were identified based on their morphological characteristics. The colonies have pin point appearance with zone of inhibition. Purified cultures were maintained on actinomycete agar slants.

Figure 2: Spectroscopic analysis of phytofabricated AgNP using actinomycetes

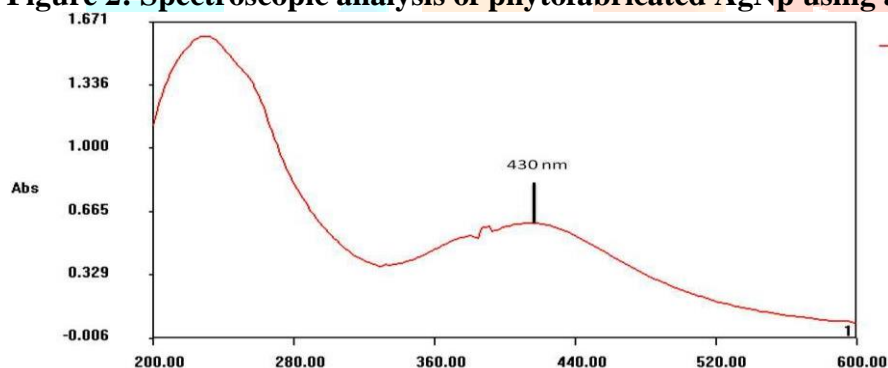
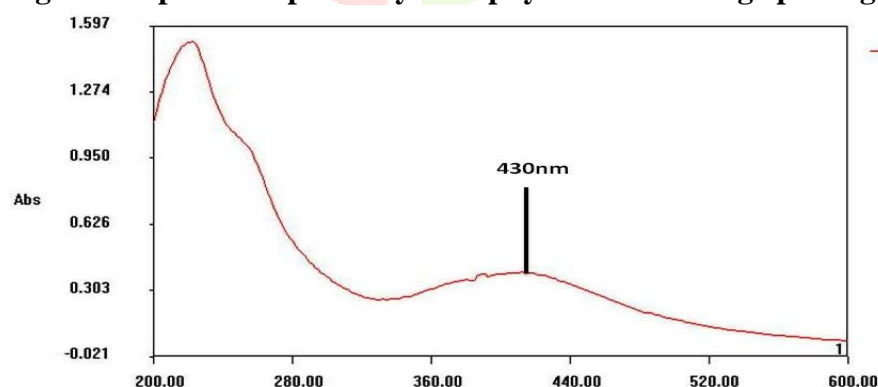


Figure 3: Spectroscopic analysis of phytofabricated AgNP using *C. taxifolia*



Uv-visible analysis of biofabricated AgNPs using *T. cordifolia* were indicated in Figure: 2 & 3. Also, the MNPs preparation using plant seed extracts has been presented, via the Ag nitrate reduction, including formation inside the plant cells [51]. The surface Plasmon peaks at 430 nm indicates the synthesis of AgNPs. Although a change in the color of Ag nitrate to yellow or yellowish-brown [50] was considered as a signal for nano-Ag consistency [52].

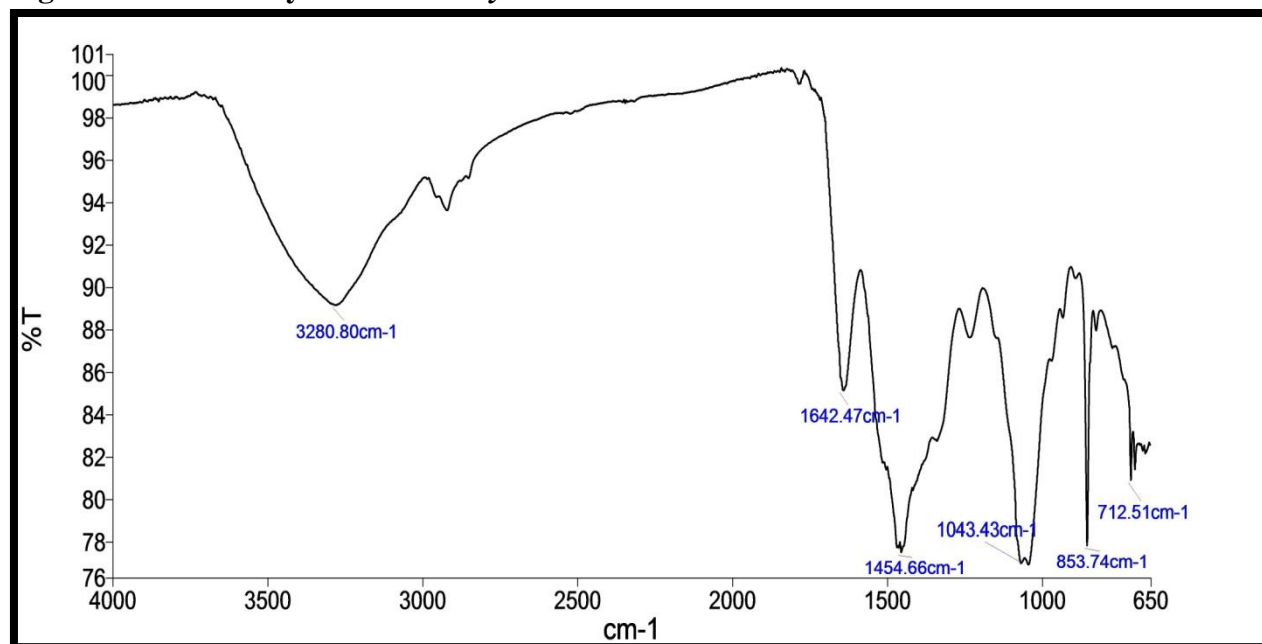
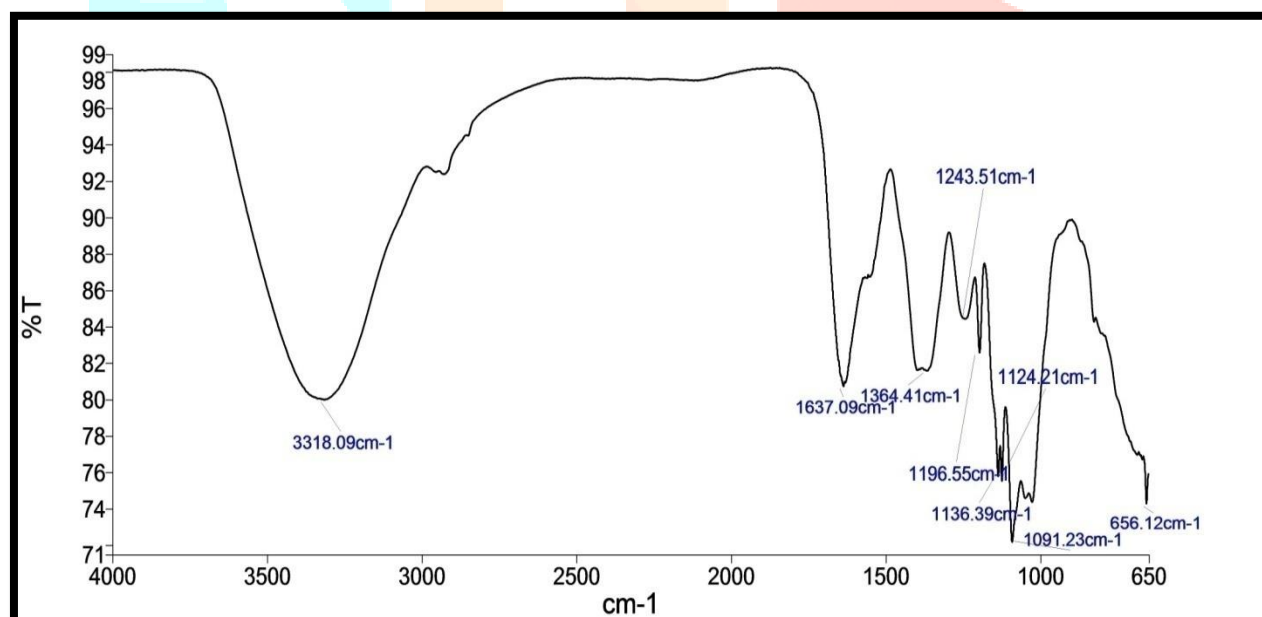
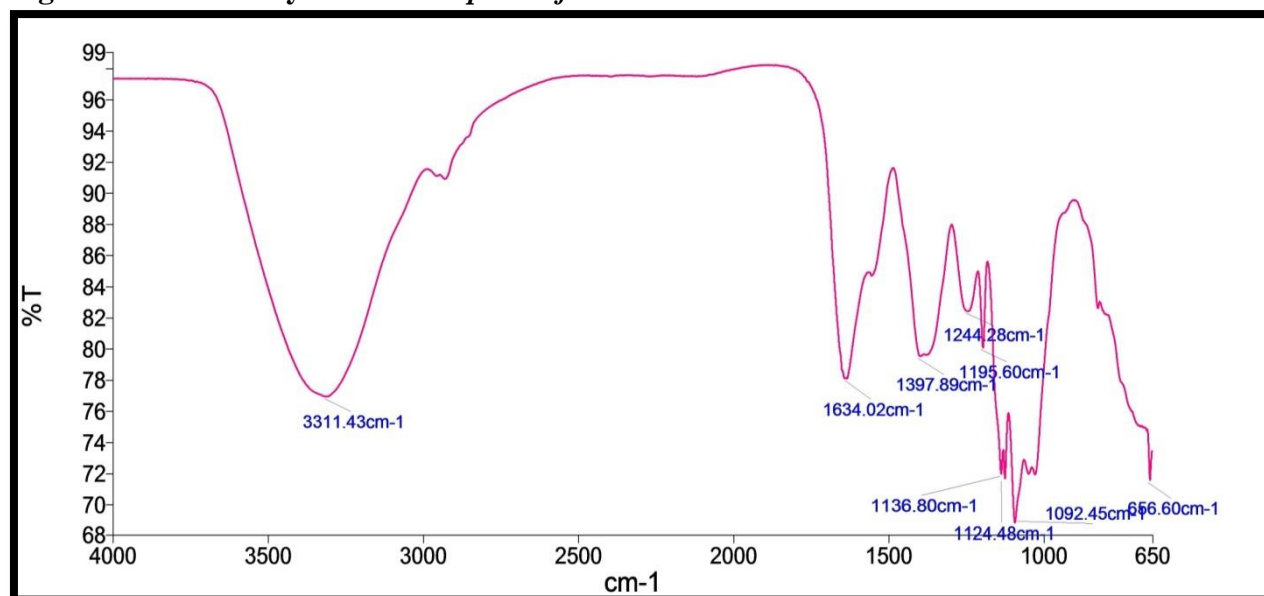
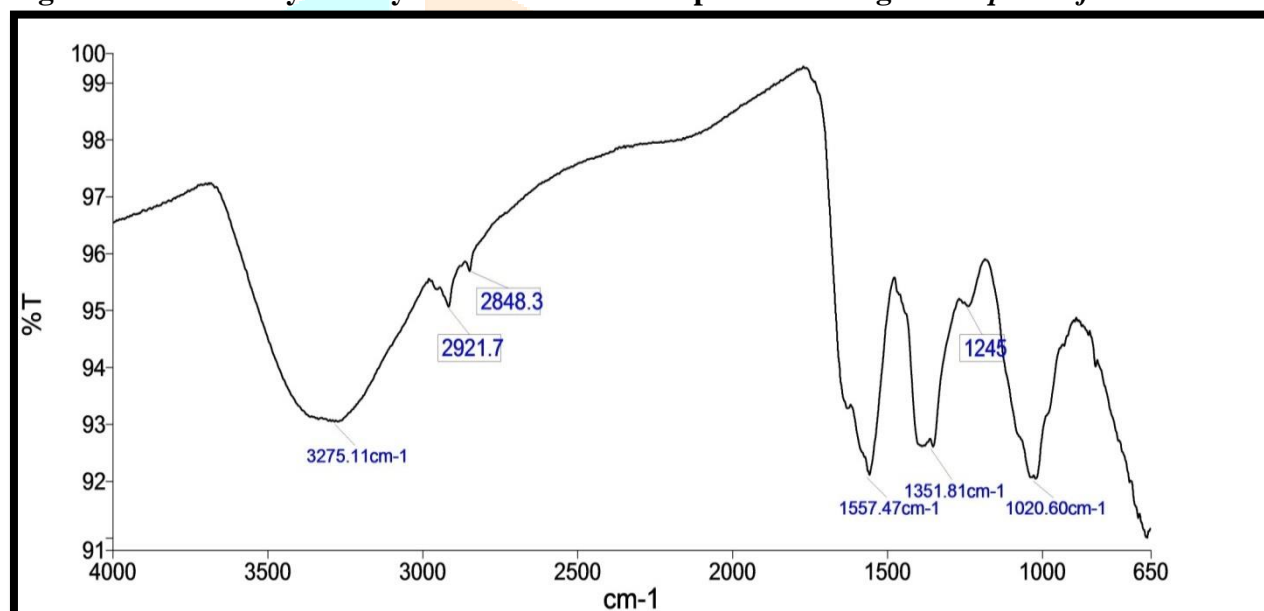
Figure 4: FTIR analysis of *Actinomyces* culture**Figure 5: FTIR analysis of synthesized silver nanoparticle using *Actinomyces***

Figure 6: FTIR analysis of *Caulerpa taxifolia* extract**Figure 7: FTIR analysis of synthesized silver nanoparticles using *Caulerpa taxifolia***

3.5 Functional assignments of phytofabricated AgNPs

FTIR analysis of actinomycetes were represented in Figure: 4. The wavenumber at 3280.80 cm^{-1} corresponds to O-H stretching of carboxylic acid. The functional assignments at 1642.47 cm^{-1} belong to C=C stretching of alkenes, spectrum at 1454.66 cm^{-1} corresponds to N-H stretching, the wavenumber at 1043.43 cm^{-1} belongs to aliphatic C-N stretching, the band at 853.74 cm^{-1} corresponds to C-H stretching, the functional assignments at 712.51 cm^{-1} corresponds to secondary amide N-H wagging. In previous studies FT-IR data demonstrated that the amide linkage of the protein possessed the higher potential to join silver and consequently forming protein covering around AgNPs to prevent agglomeration and thereby stabilize the medium [53].

FTIR analysis of biofabricated AgNPs using actinomycetes were illustrated in Figure: 5 The wavenumber at 3318.09 cm^{-1} corresponds to C=O stretching, 1364.41 cm^{-1} belongs to aromatic nitro compound NO_2 symmetric stretching, the spectral result at 1243.51 cm^{-1} , 1196.55 cm^{-1} corresponds to in-plane C-H bending, the functional assignment at 1196.55 cm^{-1} , 1124.21 cm^{-1} , 1091.23 cm^{-1} belongs to aliphatic C-O stretching, the spectrum at 1136.39 cm^{-1} corresponds to aliphatic C-N stretching, the wavenumber at 656.12 cm^{-1} belongs to =C-H bending of alkynes. Aminoacids in conjunction with carbonyl group indicate the development of a covering layer on AgNPs and thus performing as a capping agent to evade agglomeration in the aqueous medium [54]

FTIR analysis of *Caulerpa taxifolia* were depicted in Figure: 6. The wavenumber at 3311.43 cm^{-1} corresponds to Si-OH stretching, the spectral results at 1634.02 cm^{-1} confirms the presence of C=C stretching, the functional assignments at 1397.89 cm^{-1} belongs to combined C-H stretching, the wavenumber

at 1244.28 cm^{-1} indicates the presence of C-H bending, the spectrum at 1195.60 cm^{-1} , 1124.48 cm^{-1} belongs to aliphatic C-O stretching, the functional assignments at 1092.45 cm^{-1} corresponds to Si-O-C stretching, the wavenumber at 656.60 cm^{-1} belongs to secondary amide N-H wagging. Natural phenols with functional, hydroxyl [55] and carboxyl [56] groups have protonating and absorbing capabilities and catechol group of some phenolic compounds is a perfect metal absorbing moiety.

FTIR analysis of biofabricated AgNPs using *C. taxifolia* were represented in Figure: 7. The wavenumber at 3275.11 cm^{-1} corresponds to =C-H stretching of alkynes, the spectral results at 2921.7 cm^{-1} , 2848.3 cm^{-1} belongs to O-H stretching of carboxylic acids, the functional assignments at 1557.47 cm^{-1} indicates the presence of C=C stretching, the wavenumber at 1351.81 cm^{-1} confirms the presence of aromatic C-N stretching, the spectral results at 1245 cm^{-1} corresponds to C-H bending, the functional assignments at 1020.60 cm^{-1} belongs to aliphatic C-N stretching.

Figure 8: SEM micrograph of biofabricated silver nanoparticles synthesized using *Actinomyces*.

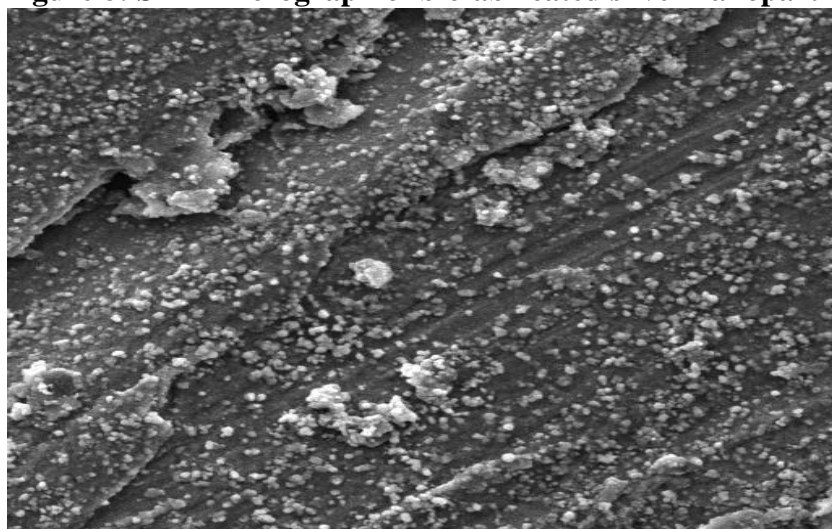
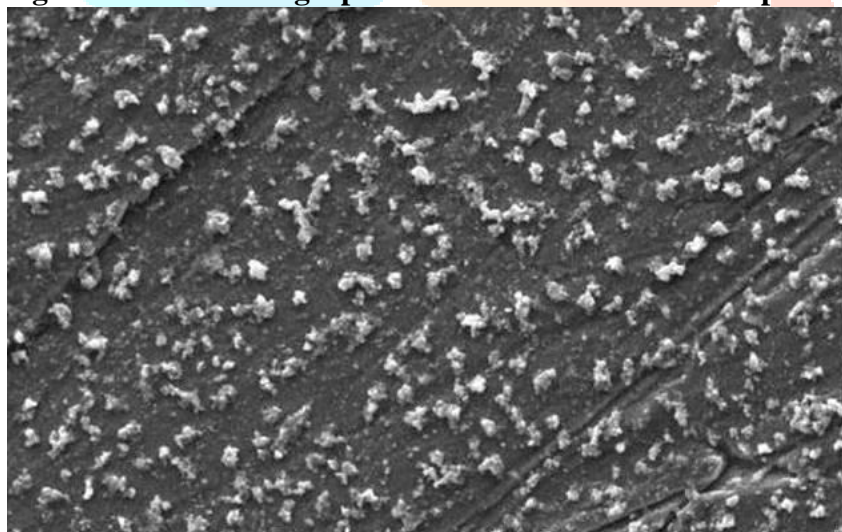


Figure 9: SEM micrograph of biofabricated silver nanoparticles synthesized using *Caulerpa taxifolia*.



3.6 SEM images of plant fabricated AgNPs

SEM micrograph of biofabricated AgNPs using actinomyces and *C. taxifolia* were depicted in figure: 8 & 9. This analysis was used to study the morphology of silver nanoparticles. Scanning electron microscopy images of the lyophilized silver nanoparticles showed mostly spherical particles of a size $10\mu\text{m}$ in range.

Figure 10: Energy dispersive x-ray diffractive (EDX) of synthesised AgNO_3 using *Actinomyces*

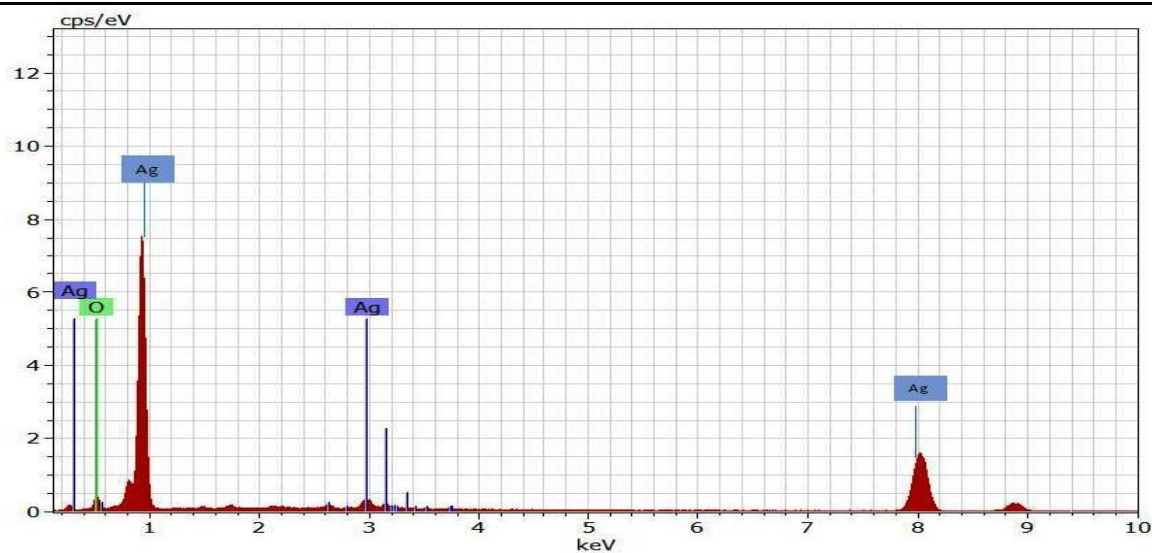
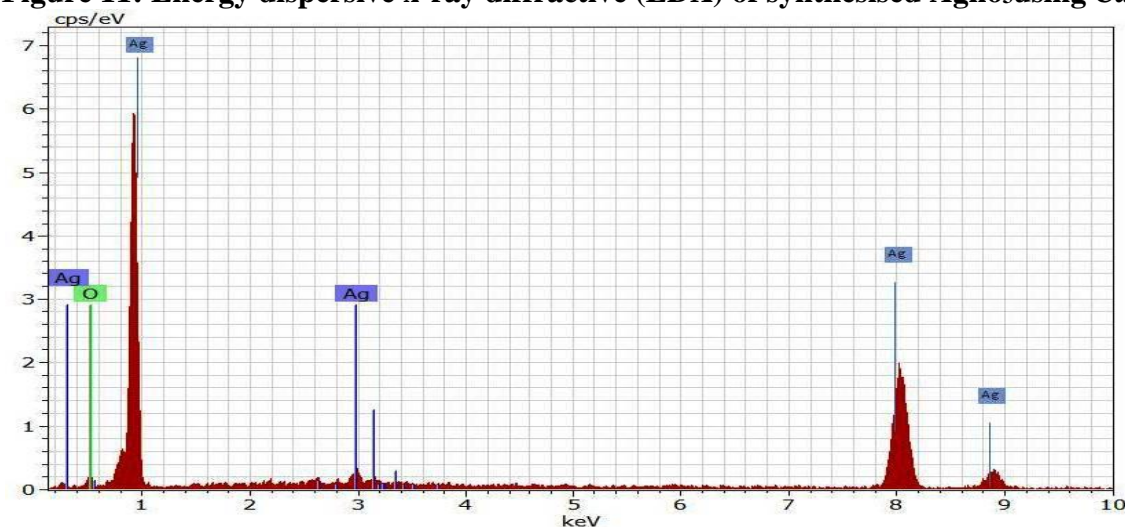
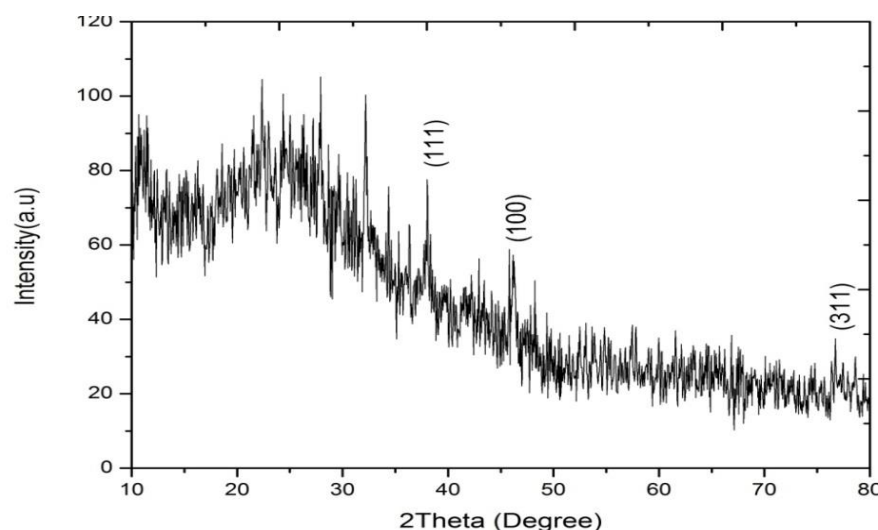
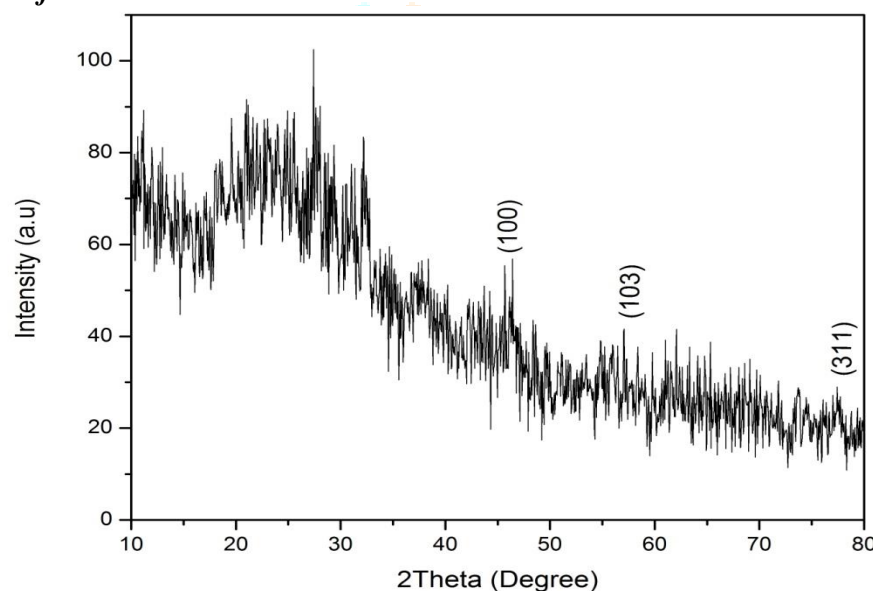


Figure 11: Energy dispersive x-ray diffraction (EDX) of synthesised AgNO₃ using *Caulerpa taxifolia*



3.7 EDX spectrum of plant fabricated AgNPs

The results of EDX spectrum of biofabricated AgNPs were depicted in Figure: 10 & 11. The composition and clarity of green synthesized AgNPs were examined using an EDX spectrometer. The EDX spectrum display elemental signals of silver atoms in biosynthesized AgNPs at around 3 keV and discovered homogenous delivery of AgNPs. Preceding reports also recommend that the EDX pattern of AgNPs normally exhibits an absorption peak nearly at 3 keV [57].

Figure 12: Representative XRD pattern of silver nanoparticles formed after reaction of *Actinomyces***Figure 13: Representative XRD pattern of silver nanoparticles formed after reaction of *Caulerpa taxifolia***

3.8 XRD pattern of plant fabricated AgNPs

XRD pattern of biofabricated AgNPs after reaction with actinomycetes and *C. taxifolia* were depicted in Figure: 12 & 13. The crystalline character of AgNPs was confirmed by XRD pattern. The diffraction peaks obtained in actinomycetes at $2\theta = 38.42^\circ$, 44.53° and 64.59° assigned to the (111), (100) and (311) planes of a face centre cubic (fcc) lattice of silver were obtained. The peaks obtained in biofabricated AgNPs using *C. taxifolia* assigned to the (100), (103), (311) planes. Presence of these peaks was due to plant extract which contains organic compounds and is responsible for the reduction of silver ions and stabilization of resultant nanoparticles [58]

IV. Conclusion

This study is the report on synthesis of biofabricated silver nanoparticles using *T. cordifolia* as reducing and capping agents. The biomolecules present in plant was identified by means of FTIR. Numerous spectroscopic and microscopic methods were used to identify the biosynthesized AgNP. Therefore it is efficiently possible to produce environmentally safe natural larvicides, which are efficient in controlling mosquito vectors of human diseases such as *Aedes aegypti*.

V. Acknowledgement

The authors would like to extend their sincere gratitude to St. Josephs College, Trichy for providing analytical facilities.

VI. Conflict of Interest

The authors declare that there is no conflict of interest

References

1. Biao, L., Tan, S., Wang, Y., Guo, X., Fu, Y., Xu, F., Zu, Y., Liu, Z. 2017. Synthesis, characterization and antibacterial study on the chitosan-functionalized Ag nanoparticles. *Mater. Sci. Eng. C*, 76: 73–80.
2. Arya, G., Kumari, R.M., Gupta, N., Kumar, A., Chandra, R., Nimesh, S. 2018. Green synthesis of silver nanoparticles using *Prosopis juliflora* bark extract: reaction, optimization, antimicrobial and catalytic activities. *Artif. Cells. Nanomed. Biotechnol*, 46: 985–993.
3. Gurunathan, S., Park, J.H., Han, J.W., Kim, J.H. 2015. Comparative assessment of the apoptotic potential of silver nanoparticles synthesized by *Bacillus tequilensis* and *Calocybe indica* in MDA-MB-231 human breast cancer cells: Targeting p53 for anticancer therapy. *Int. J. Nanomed*, 10: 4203–4222.
4. Kaur, P. 2018. Biosynthesis of nanoparticles using eco-friendly factories and their role in plant pathogenicity: a review. *Biotechnol. Res. Innov*, 2: 63–73.
5. Rajora, N., Kaushik, S., Jyoti, A., Kothari, S.L. 2016. Rapid synthesis of silver nanoparticles by *Pseudomonas stutzeri* isolated from textile soil under optimised conditions and evaluation of their antimicrobial and cytotoxicity properties. *IET. Nanobiotechnol*, 10: 367–373.
6. Ahmed, Hamed, Hoda Kabary, Mohamed Khedr and Ahmed N. 2020. Emam. Antibiofilm, antimicrobial and cytotoxic activity of extracellular green-synthesized silver nanoparticles by two marine-derived actinomycete. *RSC. Adv*, 10: 10361-10367.
7. Keshari, A.K.R., Srivastava, P., Singh, V.B., Yadav and Nath, G. 2018. Antioxidant and antibacterial activity of silver nanoparticles synthesized by *Cestrum nocturnum*. *J. Ayurveda. Integr. Med*, 11: 1–8.
8. Mallmann, E.J.J., Cunha, F.A., Castro, B.N., Maciel, A.M., Menezes, E.A., Fachine, P.B.A. 2015. Antifungal activity of silver nanoparticles obtained by green synthesis. *Rev. Inst. Med. Trop*, 57: 165–167.
9. Le Ouay, B., Stellacci, F. 2015. Antibacterial activity of silver nanoparticles: A surface science insight. *Nano. Today*, 10: 339–354.
10. Oves, M., Aslam, M., Rauf, M.A., Qayyum, S., Qari, H.A., Khan, M.S., et al. 2018. Antimicrobial and anticancer activities of silver nanoparticles synthesized from the root hair extract of *Phoenix dactylifera*. *Mater. Sci. Eng. C*, 89: 429–443.
11. Dhand, V., Soumya, L., Bharadwaj, S., Chakra, S., Bhatt, D., Sreedhar, B. 2016. Green synthesis of silver nanoparticles using *Coffea arabica* seed extract and its antibacterial activity. *Mater. Sci. Eng. C*, 58: 36–43.
12. Vazquez-Muñoz, R., Borregoi, B., Juarez-Moreno, K., et al. 2017. Toxicity of silver nanoparticles in biological systems: does the complexity of biological systems matter?, *Toxicol. Lett*. 276: 11–20.
13. Bhosale, R.S., Hajare, K.Y., Mulay, B., Mujumdar, S., Kothawade, M. 2015. Biosynthesis, characterization and study of antimicrobial effect of silver nanoparticles by *Actinomyces spp.* *Int. J. Curr. Microbiol. Appl. Sci*, 2: 144–151.
14. Mohamedin, A., El-Naggar, N.E., Hamza, S.S., Sherief, A.A. 2015. Green synthesis, characterization and antimicrobial activities of silver nanoparticles by *Streptomyces viridodiatisticus* SSHH-1 as a living nanofactory: statistical optimization of process variables. *Curr. Nanosci*. 11: 640–654.
15. Lakshmi, S.Y.S., Lakshmi, H., Sharmila, S. 2015. Isolation, screening, identification, characterization and applications of green synthesized silver nanoparticle from marine *Actinomyces-streptomyces althioticus*. *World. J. Pharm. Res*, 4(7): 1592–1611.
16. WHO, Update on the Dengue Situation in the Western Pacific Region: Northern Hemisphere Cambodia, World Health Organization, Geneva, Switzerland, 2020
17. World Health Organization, “Dengue and severe dengue,” 2017
18. Ravi, R., Zulkarnin, H., Shaida, N., et al. 2018. Evaluation of two different solvents for *Azolla pinnata* extracts on chemical compositions and larvicidal activity against *Aedes albopictus* (Diptera: Culicidae), *J Chem* 7453816: 1-8.
19. Whopes. 2016. “World Health Organization Pesticides Evaluation Scheme,”.
20. Zulkarnin, H., Shaida, N., Rozhan, N.N. et al. 2018. Larvicidal effectiveness of *Azolla pinnata* against *Aedes aegypti* (Diptera: Culicidae) with its effects on larval morphology and visualization of behavioural response. *J. Parasitol. Res*, 1383186: 1-5.
21. Ravi, R., Zulkarnin, N.S.H., Rozhan, N.N., et al. 2018. Chemical composition and larvicidal activities of *Azolla pinnata* extracts against *Aedes* (Diptera: Culicidae). *PLoS. One*, 13(11): e0206982.
22. Ravi, R., Ishak, I.H., Mohd Amin, M.F., Rasat, M.S.M., Salam, M.A., Mohd Amin, M.A. 2020. Nano-synthesized silver particles and *Azolla Pinnata* extract Larvicidal effects against *Aedes aegypti* (diptera: culicidae). *Int. J. Adv. Sci. Technol*, 29(4): 3420–3427.
23. Anonymous. 2003. Wealth of India. A Dictionary of Indian Raw Materials and Industrial Products. 1st ed. Vol. 10. New Delhi: CSIR, 251-252.

24. Vaidya, D.B. 1994. *Materia of Tibetan Medicine*. Sri Satguru Publications, New Delhi.
25. Sivakumar, V., Dhanarajan, M.S., Riyazullah, M.S. 2011. Preliminary phytochemical screening and evaluation of free radical scavenging activity of *Tinospora cordifolia*. *Int. J. Phar. Pharmaceu. Sci*, 2: 186-88.
26. Sonkamble, V.V., Kamble, L.H. 2015. Antidiabetic potential and identification of phytochemicals from *Tinospora cordifolia*. *Am J Phytomed Clin Ther* 3: 97-110.
27. Khan, M.M., dul Haque, M.S., Chowdhury, M.S. 2016. Medicinal use of the unique plant *Tinospora cordifolia* : evidence from the traditional medicine and recent research. *Asian. J. Med. Biol. Res*, 2: 508-512.
28. Birla, H., Rai, S.N., Singh, S.S., Zahra, W., Rawat, A., Tiwari, N., Singh, R.K., Pathak, A., Singh, S.P. 2019. *Tinospora cordifolia* suppresses neuroinflammation in Parkinsonian mouse model. *Neuro. Mol. Med*, 21: 42-53.
29. Harborne, J.B. 1973. *Phytochemical methods. A guide to modern techniques of plant analysis*. 1st ed. Chapman and Hall Ltd. p. 279.
30. Kumar, V., Yadav, S.C., Yadav, S.K. 2010. *Syzygium cumini* leaf and seed extract mediated biosynthesis of silver nanoparticles and their characterization. *J. Chem. Technol. Biotechnol*, 85: 1301-9.
31. NCCLS. 2010. Performance standards for antimicrobial susceptibility testing-wayne. 10th ed. NCCLS; p. M2-A8.
32. Cheesbrough, M. 2000. *District laboratory practice in tropical countries, part 2*. Cambridge University Press: Cambridge, UK, p. 434.
33. Rajakumar, G., Rahuman, A.A. 2011. Acaricidal activity of aqueous extract and synthesized silver nanoparticles from *Manilkara zapota* against *R. microplus*. *Res. Vet. Sci*, 93(1): 303-309.
34. Finney, D.J. 1971. *Probit Analysis*, 3rd edn. Cambridge University Press, Cambridge, UK.
35. Neha salaria, Sarika Sharma, Sandeep sharma. 2016. Isolation and Screening of Actinomycetes from Soil Sample of Dal Lake (Kashmir) Against Selected Pathogens. *Intl. J. Engg. Sci. Adv. Res*, 2(1):51-54
36. Stuart, B.H. *Polymer analysis*. United Kingdom: John Wiley & Sons; 2002.
37. Khan, M.M., dul Haque, M.S., Chowdhury, M.S. 2016. Medicinal use of the unique plant *Tinospora cordifolia*: evidence from the traditional medicine and recent research. *Asian. J. Med. Biol. Res*, 2: 508-512.
38. Ghosh, T., Das, A.B., Jena, B., Pradhan, C. 2015. Antimicrobial effect of silver zinc oxide (Ag-ZnO) nanocomposite particles. *Front. Life. Sci*, 8: 47-54. 952048.
39. Khan, Z.U.H., Khan, A., Chen, Y., Shah, N.S., Muhammad, N., Khan, A.U. et al. 2017. Biomedical applications of green synthesized Nobel metal nanoparticles. *J. Photochem. Photobiol. B: Biol*, 173: 150-64.
40. Khan, A.U., Yuan, Q., Khan, Z.U.H., Ahmad, A., Khan, F.U., Tahir, K., et al. 2018. An eco-benign synthesis of AgNPs using aqueous extract of Longan fruit peel: antiproliferative response against human breast cancer cell line MCF-7, antioxidant and photocatalytic deprivation of methylene blue. *J. Photochem. Photobiol. B: Biol*, 183: 367-73.
41. Khatami, M., Alijani, H., Sharifi, I. 2018. Biosynthesis of bimetallic and core shell nanoparticles: their biomedical applications: a review. *IET Nanobiotechnol. Inst. Eng. Technol*, 12(7): 879-87.
42. Mohammadine, Jad, R., Karimi, S., Iravani, S., Varma, R.S. 2016. Plant derived nanostructures: types and applications. *Green. Chem*, 18: 20-52.
43. Shakeel, M., Arif, M., Yasin, G., Li, B., Khan, A.U., Khan, F.U., et al. 2018. Hollow mesoporous architecture: a high performance Bi-functional photoelectrocatalyst for overall water splitting. *Electrochim. Acta*, 268: 163-72.
44. Singh, H., Du, J., Yi, T.H. 2017. Biosynthesis of silver nanoparticles using *Aeromonas sp.* THG-FG1.2 and its antibacterial activity against pathogenic microbes. *Artif. Cells. Nanomed. Biotechnol*, 45(3): 584-90.
45. Zhang, X.F., Liu, Z.G., Shen, W., Gurunathan, S. 2016. Silver nanoparticles: synthesis, characterization, properties, applications, and therapeutic approaches. *Int. J. Mol. Sci*. 17: E1534.
46. Kar, D., Bandyopadhyay, S., Dimri, U., Mondal, D.B., Nanda, P.K., Das, A.K. et al. 2016. Antibacterial effect of silver nanoparticles and capsaicin against MDRESBL producing *Escherichia coli*: an *in vitro* study. *Asian. Pac. J. Trop. Dis*, 6: 807-810.
47. Yuan, Y.G., Peng, Q.L., Gurunathan, S. 2017. Effects of silver nanoparticles on multiple drug-resistant strains of *Staphylococcus aureus* and *Pseudomonas aeruginosa* from mastitis-infected goats: an alternative approach for antimicrobial therapy. *Int. J. Mol. Sci*. 18: E569.
48. Allemailem, K.S., Almatroudi, A., Alsahli, M.A., Khan, A., Khan, M.A. 2019. *Tinospora cordifolia* aqueous extract alleviates cyclophosphamide-induced immune suppression, toxicity and systemic

candidiasis in immunosuppressed mice: *in vivo* study in comparison to antifungal drug fluconazole. Curr. Pharmaceut. Biotechnol, 1–5.

49. de Silva, L.L.S., Fernandes, K.M., Miranda, F.R., Silva, S.C.C., Coelho, L.C.B.B., do Navarro D.M.A.F et al. 2019. Exposure of mosquito (*Aedes aegypti*) larvae to the water extract and lectin-rich fraction of *Moringa oleifera* seeds impairs their development and future fecundity.

Ecotoxicol. Environ. Saf, 183: 1-15.

50. Mohammadinejad, R., Shavandi, A., Raie, D.S., Sangeetha, J., Soleimani, M., Hajibehzad, S.S., et al. 2019. Plant molecular farming: production of metallic nanoparticles and therapeutic proteins using green factories. Green. Chem, 21: 1845–65

51. Peralta-Videa, J.R., Huang, Y., Parsons, J.G., Zhao, L., Lopez- Moreno, L., Hernandez-Viezcas, J.A., et al. 2016. Plant-based green synthesis of metallic nanoparticles: scientific curiosity or a realistic alternative to chemical synthesis. Nanotechnol. Env. Eng, 1: 4

52. Patel, K., Bharatiya, B., Mukherjee, T., Soni, T., Shukla, A., Suhagia, B. 2017. Role of stabilizing agents in the formation of stable silver nanoparticles in aqueous solution: characterization and stability study. J. Dispers. Sci. Technol, 38: 626–31.

53. Shanmuganathan, R. et al. 2018. An enhancement of antimicrobial efficacy of biogenic and ceftriaxone-conjugated silver nanoparticles: green approach. Environ. Sci. Pollut. Res, 25(11): 1–9

54. Awwad, A.M., Salem, N.M., Abdeen, A.O. 2013. Biosynthesis of silver nanoparticles using Loquat leaf extract and its antibacterial activity. Adv. Mater. Lett, 4: 338–42.

55. Palanivel, S., Feng, L.G., Qiuqiang, Z., Palvannan, T. 2018. Flavonoids mediated ‘green’ nanomaterials: a novel nanomedicine system to treat various diseases—current trends and future perspective. Mater. Lett. 210: 26–30.

56. Anand, B.G., Dubey, K., Shekhawat, D.S., Kar, K. 2016. Capsaicin-coated silver nanoparticles inhibit amyloid fibril formation of serum albumin. Biochem, 55(24): 3345–8.

57. Wang, C., Kim, Y.J., Singh, P. 2016. Green synthesis of silver nanoparticles by *Bacillus methylotrophicus*, and their antimicrobial activity. Artif. Cells. Nanomed. Biotechnol, 44: 1127–1132.

58. Ibrahim HM. 2015. Green synthesis and characterization of silver nanoparticles using banana peel extract and their antimicrobial activity against representative microorganisms. J. Radiat. Res. Appl. Sci, 8(3): 265–75.

